

EVALUATING THE STRUCTURAL EFFICACY OF ANGLE AND CHANNEL SHEAR CONNECTORS IN BRICK AGGREGATE CONCRETE AND STONE AGGREGATE CONCRETE AND COMPARISON

Mostafa Humayun Akram^a, Md. Rabiul Alam^{a*}, Md. Naimul Haque^b, Md. Tanzim Hossain^a

^aDepartment of Civil Engineering, Chittagong University of Engineering & Technology, Chattogram-4349, Bangladesh

^bDepartment of Civil Engineering, East West University, Dhaka, Bangladesh

Article history

Received

26 March 2024

Received in revised form

27 July 2024

Accepted

28 July 2024

Published online

01 August 2024

*Corresponding author
rabiulalam@cuet.ac.bd

Graphical abstract



Abstract

Composite structure is becoming prominent for its economy, less time consumption, and higher stiffness-mass ratio. Composite action of the steel-concrete composite structure mainly depends on the connector's geometry and materials. Proper choice of shear connector could make steel beam and concrete slab cross-section minimal. This study carries out push-out tests to evaluate the structural efficiency of channel and angle shear connectors in brick aggregate concrete and stone aggregate concrete. It specifically looks at the failure mode, ductility, load-slip behavior, and energy absorption capacity. In brick aggregate concrete, results show that under monotonic loading, channel connectors have been found to have 15.27% more shear capacity & 28.38% more slip than angle connectors. Similarly, in stone aggregate concrete, channel connectors have been found to have 14% more shear capacity & 12.97% higher slip than angle connectors. On average, stone aggregate concrete has been found to have 34.84% higher shear capacity and 6.7% greater slip than brick aggregate concrete. Strain energy and plastic energy were found 78% and 17.6% less in brick aggregate specimens than those in stone aggregate specimens, respectively. Experimental results were slightly lower for both shear connectors than the empirical values.

Keywords: Push-out test, Composite structure, Failure mode, Energy absorption, Load-slip behavior

© 2024 Penerbit UTM Press. All rights reserved

1.0 INTRODUCTION

Increasing prices of building materials and labor are the main reasons for expensive housing. This is concerning for lower to middle-class earners who seek affordable housing solutions.

In Bangladesh, the people who live by the ocean are impoverished and struggle to make a safe living. Floods, tides, and tsunamis often happen in places near the ocean. Therefore, when disasters happen, the people who live near the coast have to build their houses again. This means it is imperative for them to build houses that are not expensive and will last a long time. People are trying to find faster and cheaper ways to build structures when there is an emergency. Bangladesh does not

have a lot of good-quality stones, so they have to bring stones from other places. Brick is ubiquitous in Bangladesh. Using brick aggregate in low-rise composite building construction can result in lower overall costs. Nevertheless, brick aggregate has lower durability than stone aggregate it is a cost-effective alternative material that offers both durability and strength. Composite structures are cheaper and quicker to build compared to regular RCC buildings. Using composite structures instead of RCC structures makes building 32.02% faster and saves whole expenses [1].

Low-cost sustainable housing is needed for almost all over the country. The whole country faces several types of disasters every year and the composite structures provide a solution effectively for all areas of the country.

In composite structures, the transfer of longitudinal shear between concrete and steel components is a significant factor. Three shear transfer mechanisms exist between the concrete and steel. This transfer happens through mechanical interaction, chemical bonding, and friction. While chemical bonding is often underestimated, the roles of mechanical actions and friction are of utmost importance [2]. Shear connectors are necessary to achieve mechanical action. A study by Arevalo et al. found that angle shear connectors with a 45° orientation have less scatter than those with a 90° orientation [3].

Viest [4] and Narahari [5] conducted push-out test on specimen with C-shaped shear connectors. Daniels and Crisinel [6] found that shear connectors increase mechanical–bond stresses compared to chemical–bond stresses between the deck and beam. Figure 1 (solid lines) shows typical shear resistance versus slip values, with 'ductile' and 'brittle' behaviors. Shear resistance without slip indicates chemical bonding. Pull-out test specimens, placed back-to-back, show initial erratic behavior due to slip starting at different times on each side. Shear resistance still remains after chemical bonds break due to frictional interaction between surfaces and mechanical interactions of shear keys between concrete slab and steel beam. Brittle behavior occurs when shear resistance is found to be below 0.075 N/mm². This happens in the composite body without shear keys because of little frictional and mechanical resistance that developed in the combined body, which is much lower than the chemical bond resistance of the combined body. It is often observed in decking without embossments or with small embossments. No steps are taken to eliminate chemical bonding during construction or testing of specimens. Shear resistance vs. slip values, excluding chemical bonding, are shown as dashed lines in Figure 1. In the case of brittle behavior, frictional and mechanical resistances are the last constant shear resistance after slip begins. In the case of ductile behavior, chemical bonding is a small portion of the shear-slip curve, with primary behavior assessed from the remaining curve.

Lungershausen's [7] model explains the load-bearing behavior of headed shear keys in a solid concrete slab, as shown in Figure 2. Four load-bearing components depend on the slip size (w) or thrust force (T). At low slip, flat compression struts ($\beta \leq 35^\circ$) form, supported by the bolt base and weld bead (load capacity A). Concrete pressure at the bolt base causes damage in this

area. Thrust force on the bolt shaft creates bending stress (load fraction B), leading to plastic deformations in the lower shaft area. The obstructed deformation of the dowel head creates tensile force in the shaft, balancing with compressive forces in the concrete below (load capacity component C). These compressive forces mainly occur at the bolt head on the side opposite the load. As tensile or compressive forces increase, frictional forces develop between the concrete cone and the bolt surface (load capacity fraction D). The bending load on the dowel shaft decreases with increasing tensile force. Head bolt failure in a solid concrete slab occurs through two mechanisms: concrete failure due to excessive compressive forces and bolt shearing from exceeding the tensile strength of the bolt material.

Eurocode 4 [8] provides guidelines for designing steel–concrete composite structures. In stone aggregate concrete, studies have observed the structural performance of C and V-shaped angle connectors [9], [10], [11]. Researchers [12], [13] extensively reviewed different shear connectors in composite structures.

Vianna et al. [14] conducted push–out test on T–Perfobond shear connector, studying structural response concerning shear transmission capacity, failure modes, and ductility. They also established rules for T–Perfobond connectors' design. A folded Perfobond shear key was proposed by Wang et al. [15]. The seismic performance of that key was investigated under earthquake, considering aspects for example energy dissipation, ductility, and stiffness degradation.

Bing et al. [16] developed a new fracture criterion for expecting the maximum shear capacities of the shear connectors under cyclic and monotonic loadings. Shear connectors play a crucial role in shifting shear loads to the concrete and enhancing the steel beams' load capacity.

Previous research focused on stone aggregate concrete. No studies have explored the use of brick aggregate with channel or angle shear connectors. Additionally, no comparisons exist between brick and stone aggregate concrete with these connectors in composite structures. This study aims to fill this research gap. Therefore, this study focuses on assessing the structural effectiveness of L and C-shaped connectors in brick and stone aggregate concrete.

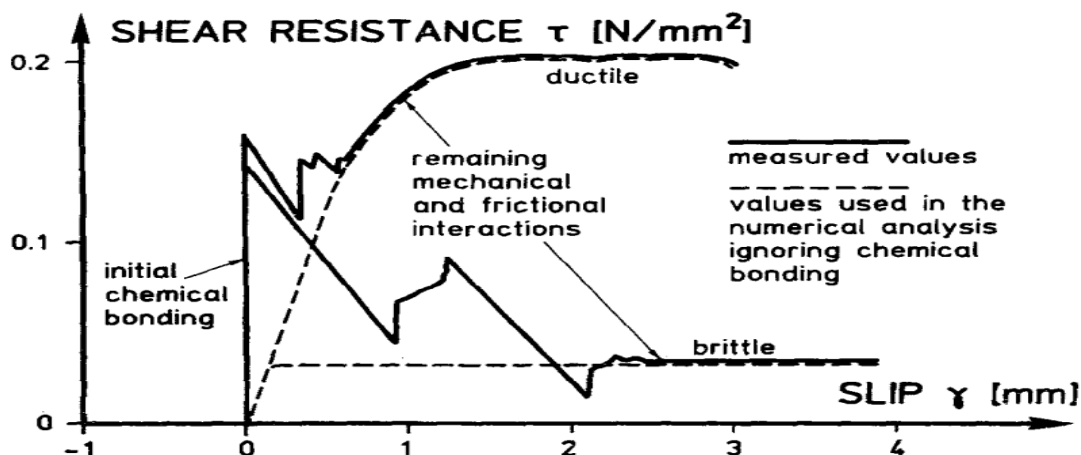


Figure 1 Shear resistance versus slip performance [6]

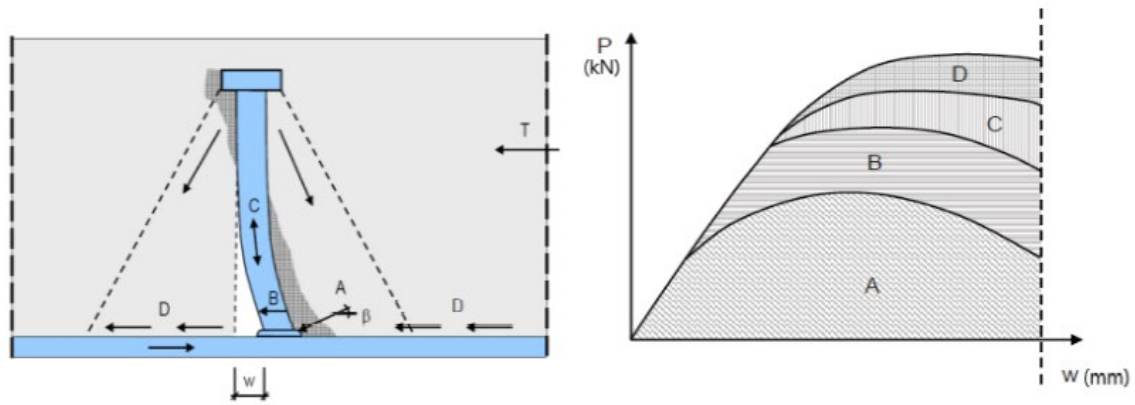


Figure 2 Load transferring process of headed shear connectors in RC slab [7]

2.0 EXPERIMENTAL INVESTIGATIONS

2.1 Resources

This study involved several tests on different materials. For both brick and stone aggregate concrete, the concrete slabs were cast using Ordinary Portland cement with an experimental compressive strength of 25 MPa. Coarse aggregates were well-graded stone and brick. For the fine aggregate, local sand was

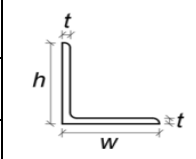
used. The properties of the coarse aggregates are shown in Table 1. The concrete slabs were cast using a mix proportion of 1:2.5:4.5, determined using the ACI mix design method [17]. Steel rebar with a yield strength of 413.69 MPa was embedded as longitudinal and tie bars in the slabs. The AISC steel construction manual [18] was not followed. The shear connectors were made separately based on practical use and measurements. In Table 2, the properties of shear connectors and wide flange steel girder are shown.

Table 1 Physical properties of coarse aggregate

Characteristics	Test value for stone aggregate	Test value for brick aggregate
Specific Gravity	2.65	1.85
Aggregate Crushing Value	38.73%	43.07%
Aggregate Impact Value	19.14%	27.46%
Los Angeles Abrasion Value	48.24%	68.82%
% Voids	50.48%	46.51%
Fineness Modulus	5.70	4.24
Unit Weight (kg/m^3)	1490	988.39
Water Absorption	0.48%	14.93%

Table 2 Shear connector & wide flange steel girder properties

Designation	Weight (kg/m)	Area (mm^2)	Web Thickness t_w (mm)	Web Height h_w (mm)	Flange Thickness t_f (mm)	Flange Width b_f (mm)	Notation
W4x13	19.35	2471	7.1	105.67	8.77	103.13	
C2x6	8.9	763.9	8.8	50.8	6.5	32	
C3x6	8.9	1135.5	9	76.2	7	40.7	

	Weight (kg/m)	Area (mm ²)	Height h (mm)	Width w (mm)	Thickness t (mm)	
L2x2x0.5	9.27	1148.38	50.8	50.8	12.7	
L3x3x0.5	13.9887	1780.642	76.2	76.2	12.7	

2.2 Preparation of Test Specimens

For the purpose of making specimens, 24 test specimens were cast in eight series. Table 3 provides an overview of all eight series. The longitudinal rebar with stirrup & shear connectors welded to the W-shaped girders is illustrated in Figure 3. The channel and angle shear connectors were welded to both beam flanges. The $\varnothing 16$ mm longitudinal bars were placed in the slab with $\varnothing 10$ mm bars as stirrups as per code specified. Two layers of longitudinal bars with stirrups were arranged in both concrete slabs. The stirrups were spaced 76.2 mm c/c with a clear cover of 12.7 mm. Each longitudinal bar was 228.6 mm apart within

the concrete slab specimen. The W-shaped girder was 304.8 mm high. Detailed dimensional measurement is shown in Figure 5.

The wooden formwork had internal dimensions of 254 mm in height, 203.2 mm in width, and 406.4 mm in length, matching the concrete slab dimensions with a clear cover. It was designed to have four sliding wooden components to close the remaining sides when the steel profile was installed, preventing the outward movement of fresh concrete. It was used to create the concrete blocks for the slabs. The formwork was removed, and the reinforced slab with the W-shaped girder was revealed, as shown in Figure 4.

Table 3 Description of test specimens

Specimens	W-shaped girders	Shear Connectors		Brick and stone aggregate concrete specimens
	Properties (mm)	Properties (mm)	Lengths (mm)	
L2	$h_w = 105.66$ $b_f = 103.12$	L-shape $h \text{ \& } w = 50.8$	50.8	3+3=6
L3	$h_w = 105.66$ $b_f = 103.12$	L-shape $h \text{ \& } w = 76.2$	76.2	3+3=6
C2	$h_w = 105.66$ $b_f = 103.12$	C-shape $h = 50.8$	50.8	3+3=6
C3	$h_w = 105.66$ $b_f = 103.12$	C-shape $h = 76.2$	76.2	3+3=6

C for channel, L for Angle, 2 & 3 to indicate shear connectors' different lengths



Figure 3 Longitudinal rebar with stirrup, shear connectors along with girders [L2, L3, C2, C3]

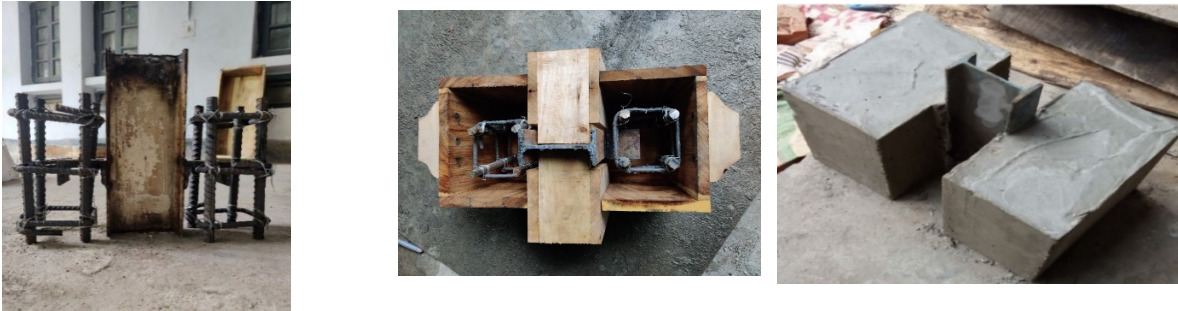


Figure 4 W-shaped girder along with reinforced steel, formwork, and concrete slab specimen

2.3. Instrumentation and Testing Procedure

A total of 24 push-out tests (12 for brick aggregate concrete and 12 for stone aggregate concrete) were conducted using a Universal Testing Machine. The model no. of Universal Testing Machine is TUN-2000. It is manufactured by Fine Spavy

Associates & Engineers Pvt. Ltd., India. Test was carried out by following the design standards of British BS5950 [19]. Figure 5 and Figure 6 display the schematic diagram of the specimen and arrangements of the test, respectively.

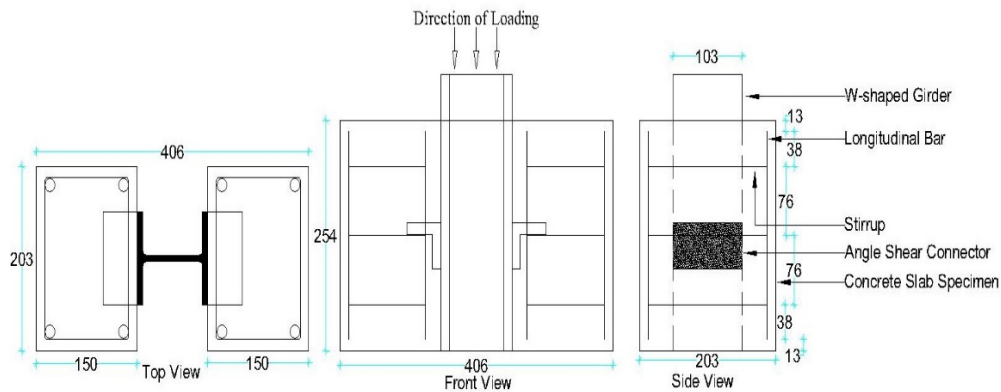


Figure 5 Schematic diagram of the specimen

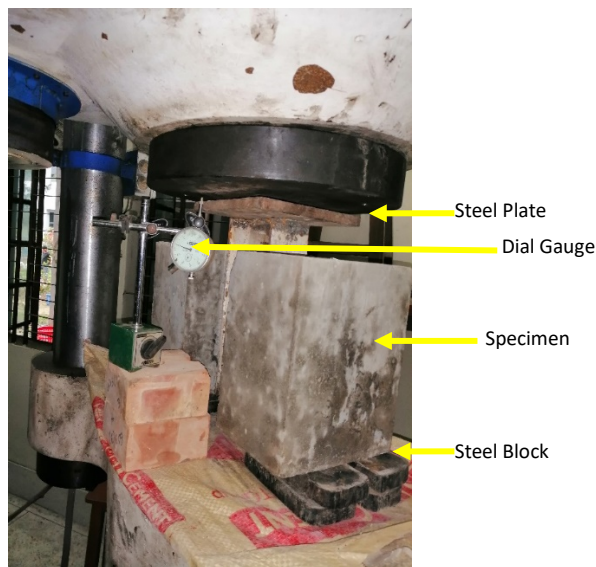


Figure 6 Arrangement of specimen in Universal Testing Machine

3.0 OUTCOMES

3.1 Load-slip Behavior

Figure 7 shows the average load-slip diagrams of all eight series. Both brick and stone aggregate concrete specimens show a similar trend in results. The strength of the connectors rises as the length increases. As the load increases, the slip value also increases until it reaches an ultimate shear load. Then the load decreases, but deformation continues until the slab fails completely. After surpassing the maximum shear load, the load-bearing strength diminishes rapidly. Short-length shear connectors (L2 and C2) have flatter curves, while longer lengths have a combination of stiff and flat curves, indicating higher initial stiffness. The shear connectors exhibit varying degrees of slip at the maximum shear load for both categories of concrete slabs. The maximum shear strength and slip amounts are calculated and contrasted to gain a precise understanding of the load-slip characteristics. Table 4 and Table 5 compare the maximum shear and slip values of different shear connectors.

Steel Concrete Composite Made with Brick Aggregate:

The C3 specimen for C-shape connectors (Channel shear connectors) carries an average load of 134 kN, while the C2 specimen carries 115 kN, resulting in a 14.18% decrease in ultimate shear capacity. The L3 specimen carries a mean load of 112 kN, while the L2 carries 104 kN, resulting in a 7.14% decrease in ultimate shear capacity. This decrease in shear capacity was due to the shorter length of angle shear connectors concentrating the force on a smaller section.

The C3 specimen exhibits greater flexibility compared to the C2 specimen. At the highest load, the C3 specimen (having 8.5 mm of slip) has 35.5% more slip than the C2 specimen (having 6.2 mm of slip). However, the L2 specimen is more flexible than the L3 specimen. At the maximum load, the L2 specimen (having 7.8 mm of slip) has 113.7% more slip than the L3 specimen (having 3.65 mm of slip).

The uneven bottom surface of one slab (the height of one end with respect to other end) of specimen L3 was found the main reason for showing a small amount of slip. It happened during the casting of specimen L3 (faulty placement of shutter) that could not be minimized by grinding only. In this case, compressive load acted in an eccentric manner. Therefore, one corner of specimen L3 broke quickly (Figure 8) and the slip value was small. It was actually a specimen preparation fault which could not be expected. Furthermore, in stone aggregate slab, the slip at the maximum breaking load of L2 and L3 specimens is less than those obtained in the C2 and C3 specimens, respectively.

However, the total slip value of L2 specimen was found little more than the slip of C2 specimen. After reaching the peak load, strain softening starts and many factors such as failure mode, aggregate size and proportion, uniformity of specimen, etc., are involved in the entire failure of the specimen. These factors could vary from specimen to specimen. It is worth mentioning that the entire test was done under a load-controlled method. The load was increased at regular intervals and slip values were taken at each load value.

Figure 7(a) displays load-slip curve for concrete slab made with brick aggregate. The channel connectors have a larger shear capacity than the angle connectors of the same length. The L3, C3, C2, and C3 specimens have shear capacities that are 7.70%, 16.50%, 10.60%, and 19.60% higher than the L2, C2, L2, and L3 specimens, respectively. The slip of the C2 specimen and C3 specimen is 21% lower and 130% higher than the L2 specimen and L3 specimen, respectively.

Steel Concrete Composite Made with Stone Aggregate:

In case of L-shape shear connectors, the L2 specimen carries an average load of 140 kN while the L3 specimen carries an average load of 153 kN (an increase of 9.30% in the ultimate shear capacity). A similar trend is valid in case of a C-shape shear connector. For the ultimate shear capacity, C3 specimens are 8.75% higher than C2. Again, C2 specimens are 14.30% higher than L2 specimens. C3 specimens are 13.70% higher than L3 specimens.

Like the shear capacity, the slip value increases with an increase in length, and the C-shape shear connector experiences higher slip than the L-shape shear connector. However, the slip value increases nominally. For the slip, L3, C3, C2, and C3 are 26%, 27.7%, 12.07%, and 13.69% larger than L2, C2, L2, and L3, respectively. However, the load percentage increased in load cases much higher than those obtained in slip values. Figure 7(b) displays the load-slip curve for the stone aggregate concrete slab.

For the ultimate shear capacity of stone specimen L2, L3, C2, and C3 are 34.6%, 36.6%, 39.13%, and 29.85% higher than brick specimen, L2, L3, C2, C3, respectively. Again, for the ultimate shear capacity of stone specimen C2, C3, L2, and L3 are 53.85%, 55.36%, 21.74%, and 14.18% higher than brick specimen, L2, L3, C2, and C3, respectively. For the slip, stone specimens, L2, C3, C2, L2, and L3 are 25.64%, 1.19%, 16.67%, 6.45%, and 13.1% lower than brick specimen, L2, C3, L2, C2, and C3 respectively. Again, stone specimens, L3, C2, and C3 are 100%, 4.84%, and 127.39% higher than brick specimen, L3, C2, and L3, respectively.

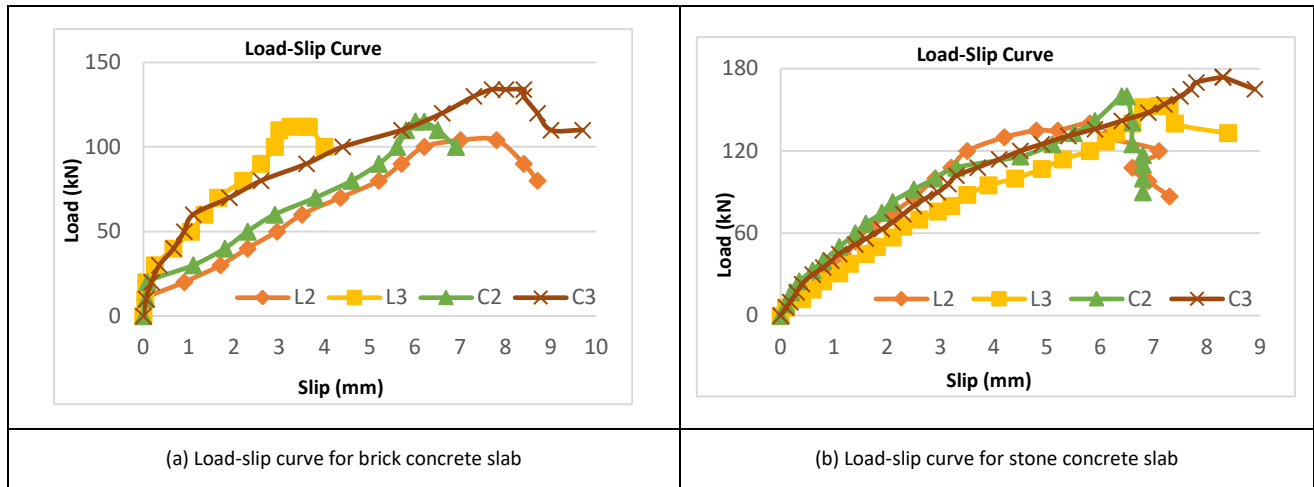


Figure 7 Variation of Load-slip for different shear connectors



Figure 8 Broken specimen made with brick aggregate L3 after loading

Table 4 Evaluation of maximum shear capacity of shear connectors

Specimen	Shear Capacity (kN)				% difference between L & C		% difference between specimen _2 & _3				% difference between			
	Brick		Stone		Brick	Stone	Brick		Stone		(1) & (3)	(2) & (4)	(1) & (4)	(2) & (3)
	(1)	(2)	(3)	(4)			L	C	L	C				
	L	C	L	C										
_2	104	115	140	160	+10.6	+14.3					+34.6	+39.13	+53.85	+21.74
_3	112	134	153	174	+19.6	+13.7	+7.7	+16.5	+9.3	+8.8	+36.6	+29.85	+55.36	+14.18

Table 5 Evaluation of maximum slip of shear connectors

Specimen	Slip (mm)				% difference between L & C		% difference between specimen _2 & _3				% difference between			
	Brick		Stone		Brick	Stone	Brick		Stone		(1) & (3)	(2) & (4)	(1) & (4)	(2) & (3)
	(1)	(2)	(3)	(4)			L	C	L	C				
	L	C	L	C										
_2	7.8	6.2	5.8	6.5	-21	+12.07					-25.6	+4.84	-16.67	-6.45
_3	3.65	8.5	7.3	8.3	+130	+13.69	-53	+35.5	+26	+27.7	+100	-1.19	+127.39	-13.1

3.2 Energy Absorption

In this study, measuring the energy absorption of specimens with L-shaped and C-shaped shear connectors was focused on.

To do this, the load-slip variation curves of these specimens were made. The amount of energy absorbed by the connectors was determined by calculating the area under the curve. On average, strain energy and plastic energy were found 78% and

17.6% less in brick aggregate specimens than those in stone aggregate specimens, respectively.

It was found that energy absorption in both plastic-strain cases occurred in the tested specimens. However, the energy absorption in the plastic case was higher than the strain energy absorption in both types of connectors. This suggests that the connectors have the ability to deform and absorb a significant amount of energy before reaching their ultimate failure point.

Interestingly, the strain energy absorption in brick aggregate specimens was observed as minimal. This could be due to the inherent stiffness and brittleness of brick, resulting in less ability to deform under load and dissipate energy.

Additionally, it was noted that in stone aggregate specimens, the strain energy absorption was more negligible in channel

connectors compared to angle connectors. This could be attributed to the different geometries and structural characteristics of these connectors, leading to variations in their deformation and energy absorption capabilities.

Overall, these findings contribute to the understanding of the energy absorption properties of different types of shear connectors. The results emphasize the importance of considering both strain and plastic energy absorption in the design and analysis of structures employing such connectors, as well as the influence of aggregate type and connector geometry on their energy absorption capabilities. Figure 9 illustrates the energy absorption curve.

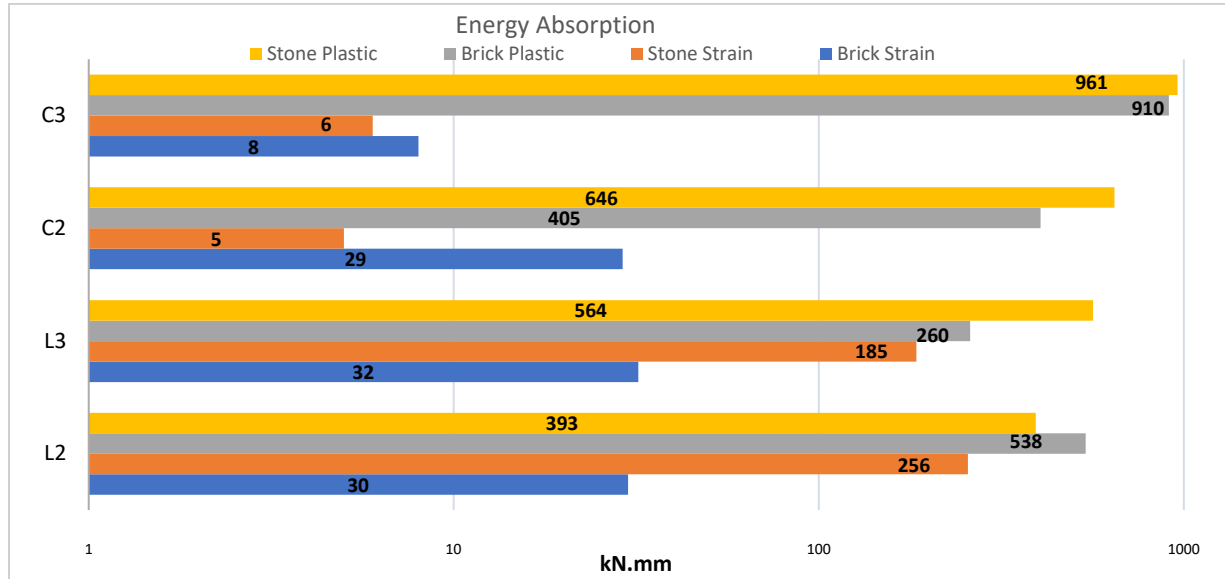


Figure 9 Energy absorption

3.3 Comparison of Experimental and Theoretical Value

Since it is not always feasible to conduct tests, theoretical equations are necessary to create and assess the ability of shear connectors to handle shear forces. A few formulas for calculating the expected shear strength of C-shaped connectors have already been established by AISC [20] and National Building Code, Canada (NBC) [21]. O. and Kiyomiya [22] created a practical equation to determine the theoretical shear strength of L-shaped connectors for shear purposes. Table 6 provides the mathematical equations with the explanation of notations of these references. In order to compare experimentally determined results with the referenced formulas for checking the effectiveness of the results, a comparison is made between the measured shearing forces and shearing forces obtained from

the theoretical determination of the reference formulas, as shown in Figure 10. It is evident that the shear values obtained by the AISC closely match with an error of 1.54% and -1.26% to the shear values obtained from C3 stone aggregate specimens and C2 brick aggregate specimens, respectively. Furthermore, C3 brick aggregate specimens' and C2 stone aggregate specimens' shear values satisfy reasonably with an error of 27.11% and -26.38% to the shear values obtained by the AISC, respectively. C3 specimens for both stone and brick aggregate shear values satisfy reasonably with shear values obtained from the NBC formula. Other measured values do not match satisfactorily with the theoretical values.

Table 6 Formulas for calculating shear capacity of the angle & channel connectors

Shear connector	Formulations for determining nominal shear capacity (kN)		
	AISC-2005 [20]	NBC [21]	Kiyomiya and Yokota [22]
Angle	-----	-----	$P = 65\sqrt{t_w}L_c\sqrt{f'_c}$
Channel	$Q_n = 0.3(t_f + 0.5t_w)L_c\sqrt{f'_c E_c}$	$Q_n = 36.5(t_f + 0.5t_w)L_c\sqrt{f'_c}$	-----

In Table 6, L_c = shear connectors' length, E_c = concrete's elasticity modulus, P = nominal shear of angle connector, Q_n = nominal shear of channel connector, t_f = flange thickness of shear

connector, f_c' = concrete's cylindrical compressive strength, t_w = shear connector's web thickness.

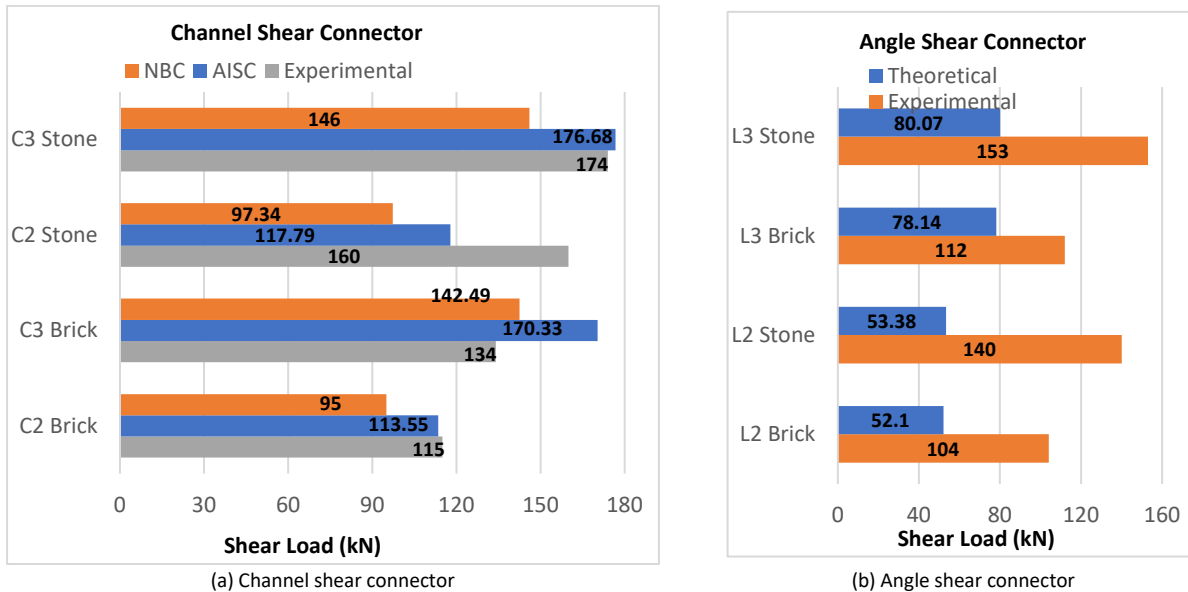


Figure 10 Experimental ultimate and theoretical nominal shear capacity of the shear connectors

3.4 Patterns of Failure

The ways in which push-out test specimens fail include connector yielding and fracture, crushing and splitting of concrete of connecting slab, shear failure, and shear and bending combined failure. The failure modes of angle and channel shear connectors were found to be nearly the same in both brick and stone aggregate concrete. In the fractured surface of brick and stone aggregate concrete, there is no significant difference in failure patterns. However, little variation of fractured surfaces was observed in the concrete slab. In the concrete slab made with brick aggregate, aggregate crushing in addition to mortar failure was observed more than those observed in the slab made with stone aggregate. Mortar failure was found as dominant failure for both brick and stone aggregate concretes. However, the channel connectors broke faster than the angles for both kinds of concrete slabs. Over time, this crack continued to grow and eventually caused the specimen to fracture as the deformation increased completely. Connectors that yield under heavier weights were detected in most of the tests. The failure characteristics of both kinds of

specimens are similar. There are cracks in the lower part of the slab after the shear connectors.

The cracks begin as an inclined shearing fracture when applied to the load, and as the force rises, it extends along the depth of the concrete block (horizontal direction). As the weight increases, the inclined crack transforms into a vertical crack that runs parallel to the slab upward until it reaches the bottom. When the shear load reaches its maximum point, the cracks widen significantly, and the concrete close to the shear connectors on the side is crushed. Consequently, the solid block is divided into two separate sections (lower and higher sections).

The illustration in Figure 11 shows the failure outline of damaged specimens of C3 and L3. The destruction on the edge of the concrete slab can be seen in those images. In brick aggregate concrete slabs, crack failure typically happens for both shear connectors. Regarding stone aggregate concrete slabs, when it comes to L-shaped and C-shaped shear connectors, most of the specimens primarily undergo failure due to shear, except for a few instances. Following the collapse event, it was observed that there was an increased occurrence of cracking in channels compared to angles for both types of concrete slabs.



Figure 11 Test specimens' failure patterns

4.0 CONCLUSIONS

This study specifically focuses on the usage of shear connectors between brick aggregate concrete and stone aggregate concrete. It was found that the concrete specimens made with stone aggregate were stronger compared to those made with brick aggregate and also channel shear connectors are more effective than angle shear connectors in transferring horizontal shear.

Bricks are abundantly available throughout Bangladesh, making them a more cost-effective choice. Using brick aggregate in composite structures not only reduces the total building cost but also saves time and manpower. Additionally, it helps in reducing the load on the foundation.

It is important to note that while brick aggregate is suitable for low-rise buildings, it is not recommended for high-rise constructions due to its limitations. However, where low-rise buildings (2-3 stories) with shallow foundations are common, the usage of brick aggregate concrete can considerably reduce the overall construction cost. This makes it a viable option for affordable housing. The core discoveries are given below:

- The shear connectors' length and type have an impact on the ultimate shear capacity and slip of low-strength brick aggregate and stone aggregate concrete slabs. The failure mode did not vary with different lengths and types of connectors.

- The channel shear connectors in both concrete slabs had a larger shear capacity than the angle shear connectors of the same length.

- There is a direct relationship between the length of the shear connector and the shear capacity, as an increase in length results in an increase in shear capacity.

- Maximum shear capacity and slip found in a C-shape shear connector with a length of 76.2 mm were 174 kN and 8.3 mm, respectively, in the stone aggregate concrete slab, whereas in brick aggregate concrete, it was found as 134 kN and 8.5 mm.

- The failure modes of all shear connectors were found to be ductile, meaning they do not fail abruptly but rather show signs of deformation before failure. Additionally, the ductility of the specimens increased as the length of the connectors increased.

- Regarding energy absorption, plastic energy absorption was found to be greater than strain energy absorption. Nevertheless, in the case of brick concrete slabs, strain energy absorption was found to be too low. Furthermore, the channel connector in stone concrete slabs exhibited lower strain energy absorption compared to the angle connector. On average, strain energy and plastic energy were found 78% and 17.6% less in brick aggregate specimens than those in stone aggregate specimens, respectively.

- The experimental shear force values reasonably satisfy the shear force values obtained from theoretical determination except the channel shear force values obtained from the Kiyomiya and Yokota.

- In terms of failures observed, every specimen showed signs of shear failure, split failure, and crushing failure of the concrete slab. This indicates the various ways in which the RC slab can fail under different load conditions.

Acknowledgments

The research described in this paper has been conducted with funding from the Department of Civil Engineering at Chittagong University of Engineering & Technology (CUET).

References

- [1] B.L. Rajput, M.A. Hussain, N.N. Shaikh, J. Vadodaria, 2013. Time and Cost Comparison of Construction of RCC, Steel and Composite Structure Building. *IUP Journal of Structural Engineering*. 6(4): 49–59.
- [2] M.R. Salari, E. Spacone, P.B. Shing, D.M. Frangopol, 1998. Nonlinear Analysis of Composite Beams with Deformable Shear Connectors, *Journal of Structural Engineering*. 124: 1148–1158. [https://doi.org/10.1061/\(ASCE\)0733-9445\(1998\)124:10\(1148\)](https://doi.org/10.1061/(ASCE)0733-9445(1998)124:10(1148)).
- [3] D. Arévalo, L. Hernández, C. Gómez, G. Velasteguí, E. Guaminga, R. Baquero, R. Dibujés, 2021. Structural performance of steel angle shear connectors with different orientation, *Case Studies in Construction Materials*. 14: e00523. <https://doi.org/10.1016/j.cscm.2021.E00523>.
- [4] I.M. Viest, C.P. Siess, J.H. Appleton, N.M. Newmark, 1951. Full-scale tests of channel shear connectors and composite t-beams, *Studies of Slab and Beam Highway Bridges, Part IV*. University of Illinois at Urbana Champaign, University of Illinois Engineering Experiment Station, Bulletin Series No. 405.
- [5] R.S. Narahari, 1970. Composite Construction - Tests On Small-Scale Shear Connectors, *Inst Engrs Civil Eng Trans /Australia/*. 12(1): 106–115.
- [6] [6] B.J. Daniels, M. Crisinel, 1993. Composite Slab Behavior and Strength Analysis. Part I: Calculation Procedure, *Journal of Structural Engineering*. 119: 16–35. [https://doi.org/10.1061/\(ASCE\)0733-9445\(1993\)119:1\(16\)](https://doi.org/10.1061/(ASCE)0733-9445(1993)119:1(16)).
- [7] Lungershausen, 1988. H.: Zur Schubtragfähigkeit von Kopfbolzendübeln, Mitteilung Nr. 88-7, Institut für konstruktiven Ingenieurbau, Ruhr-Universität Bochum, Dissertation.
- [8] N. Europeenne, 2004. EUROPEAN STANDARD Eurocode 4: Design of composite steel and concrete structures-Part 1-1: General rules and rules for buildings.
- [9] A. Shariati, N.H. Ramli Sulong, M. Suhatri, M. Shariati, 2012. Investigation of channel shear connectors for composite concrete and steel T-beam, *International Journal of the Physical Sciences*. 7(11): 1828–1831. <https://doi.org/10.5897/IJPS11.1604>.
- [10] M. Shariati, N.H. Ramli Sulong, A. Shariati, M.A. Khanouki, 2016. Behavior of V-shaped angle shear connectors: experimental and parametric study, *Materials and Structures*. 49: 3909–3926. <https://doi.org/10.1617/S11527-015-0762-8>.
- [11] M. Shariati, N.H. Ramli Sulong, H. Sinaei, M.M. Arabnejad.Kh, P. Shafiq, 2011. Behavior of Channel Shear Connectors in Normal and Light Weight Aggregate Concrete (Experimental and Analytical Study), *Advanced Materials Research*. 168–170: 2303–2307. <https://doi.org/10.4028/WWW.SCIENTIFIC.NET/AMR.168-170.2303>.
- [12] R.T. Pardeshi, Y.D. Patil, 2021. Review Of Various Shear Connectors In Composite Structures, *Advanced Steel Construction*. 17(4): 394–402. <https://doi.org/10.18057/IJASC.2021.17.4.8>.
- [13] A. Shariati, N. H. Ramli Sulong, M. Suhatri, M. Shariati, 2012. Various types of shear connectors in composite structures: A review, *International Journal of the Physical Sciences*. 7(22): 2876–2890. <https://doi.org/10.5897/ijpsx11.004>.
- [14] [14] J. da C. Vianna, L.F. Costa-Neves, P.C.G. da S. Vellasco, S.A.L. de Andrade, 2008. Structural behaviour of T-Perfobond shear connectors in composite girders: An experimental approach, *Engineering Structures*. 30(9): 2381–2391. <https://doi.org/10.1016/j.engstruct.2008.01.015>.
- [15] [15] Z.S. Wang, H.Q. Qin, Y. Yang, Y.H. Liu, H.C. Guo, J.B. Tian, 2022. Study of bond-slip performance and ultimate bearing capacity calculation under static and reciprocating action of folded perfobond shear keys, *Case Studies in Construction Materials*. 17: e01347. <https://doi.org/10.1016/j.cscm.2022.e01347>.
- [16] B. Lu, C. Zhai, S. Li, W. Wen, 2019. Predicting ultimate shear capacities of shear connectors under monotonic and cyclic loadings, *Thin-Walled Structures*. 141: 47–61. <https://doi.org/10.1016/j.tws.2019.04.002>.
- [17] A. ACI, 2009. 211.1-91 (Reapproved 2009) Standard practice for selecting proportions for normal, heavyweight, and mass concrete.

- [18] ANSI/AISC 360-10, 2010. Specification for Structural Steel Buildings. Approved by the AISC Committee on Specifications.
- [19] P. BS5950, 1990. 3-1, *Structural use of steelwork in building: Code of practice for design of simple and continuous composite beams*, London: British Standards Institution.
- [20] ANSI/AISC 360-05, 2005. Specification for Structural Steel Buildings. Approved by the AISC Committee on Specifications and issued by the AISC Board of Directors.
- [21] National building code of Canada, 2005. Issued by the Canadian Commission on Building and Fire Codes., Institute for Research in Construction (Canada), 12th Edition.
- [22] O. Kiyomiya, H. Yokota, 1986. Strength of shear connector by shape steel in composite member with steel and concrete, in: *Proc. of Symposium on Research and Application of Composite Constructions, Japan Society of Civil Engineers*. 113–118.